Journal of Geochemical Exploration 161 (2016) 62–71

Contents lists available at ScienceDirect

Journal of Geochemical Exploration

journal homepage: www.elsevier.com/locate/gexplo

Fractal analysis of geochemical landscapes using scaling noise model

Guoxiong Chen [a,b,c], Qiuming Cheng [a,b,c,*], Renguang Zuo [a]

[a] State Key Laboratory of Geological Processes and Mineral Resources, China University of Geosciences, Wuhan 430074, China
[b] Faculty of Earth Resources, China University of Geosciences, Wuhan 430074, China
[c] Department of Earth and Space Science and Engineering, York University, Toronto M3J 1P3, Canada

ARTICLE INFO

Article history:
Received 20 October 2015
Accepted 8 November 2015
Available online 10 November 2015

Keywords:
Fractals
Spectral analysis
Scaling exponent
Persistence
Geochemical anomaly

ABSTRACT

Fractal/multifractal concepts have facilitated the description and analysis of complex geochemical data in both mineral exploration and environmental studies. Scaling ($1/f^{\beta}$) noise has been ubiquitously found in geosciences but lack in-depth studies for geochemical distribution pattern in mineral exploration. In the present paper, the $1/f$ scaling natures of geochemical landscapes are investigated using spectral method through geochemical samples in stream sediments from Nanling Range, China. The results show explicit differences in scaling exponent (β) between major elements and trace elements, between highly enriched elements (e.g., W, Sn, Mo and Bi) and relatively low enriched elements (e.g., Au, Ag and Cu), where β measures the strength of persistence (or the degree of roughness) of geochemical landscapes. Furthermore, fractal mapping of geochemical patterns (W and Sn element) is undertaken to reveal the spatial association between local fractal dimension and mineralization. The finding is that most of the W and Sn deposits in study area exhibit rough geochemical patterns with fractal dimension ranging from 2.3 and 2.7 ($2.6 \le \beta \le 3.4$). We proposed to recognize the complex geochemical anomalies containing both stochastic (irregular) and deterministic (regular) components from fractal noise perspective.

1. Introduction

Fractal geometry was introduced and popularized by Mandelbrot (1967, 1989) to describe complex natural objects showing similar geometries over a variety of scales. This fractal/scaling nature, resulting from the combination of regular (deterministic) and irregular (stochastic) factors, is commonly characterized with fractal dimension that is non-integer greater than or less than the integer Euclidian dimension. The past 40+ years have seen the extensions of fractal theory from geometries to fields that significantly increase its applicability. Fractality (self-affinity) generally follows power-law type relations associated with scale-invariance that can be represented as straight line on a log–log paper. The scale-invariant processes broadly exist in geosciences (Turcotte, 1997; Cheng, 2008), such as earthquakes, floods, hurricanes, volcanoes, rains and clouds. Recent studies suggest that mineralization in the crust could be considered as one type of scale-invariant geoprocess (Cheng, 2008), and ore deposits resulting from huge accumulation of metal elements often generate singular geochemical distribution which manifests fractal/multifractal natures.

Geochemical exploration have found with increasingly interests and benefits of using fractal (power-law) models to characterize geochemical distribution, including concentration–area (C–A) model (Cheng et al., 1994; Cheng, 2012), concentration–distance (C–D) model (Li et al., 2003), and concentration–volume (C–V) model (Afzal et al., 2011; Afzal et al., 2013), to name but a few examples. These fractal models are particularly useful for handling geochemical data including the separation and identification of geochemical anomalies, thereby assisting in mineral exploration (Cheng et al., 1994; Cheng, 2007). Local singularity analysis (LSA) is a well-known example of using density-area fractal model for weak information extraction by mapping the spatial distribution of local singularity strength (local fractal dimension) for complex geochemical landscapes (Cheng, 2008, 2012). Several case studies have demonstrated that the LSA or singularity mapping method is a powerful tool for discovering concealed ore deposits as well as other buried geological bodies (Cheng, 2006, 2007; Zuo et al., 2009; Agterberg, 2014a; Chen et al., 2015).

The scaling ($1/f$) noise/process has been widely found in the nature, depicting that the power density spectrum, $S(f)$, of self-affine time series scales as a power-law of the frequency ($1/f^{\beta}$). The spectral analysis is a commonly used method to study the $1/f$ scaling nature of geofields in the Fourier domain (see e.g., Huang and Turcotte, 1989; Malamud and Turcotte, 1999), and the scaling exponent (β) can measure the strength of persistence, namely, the correlations between adjacent values within the time or spatial series. Lovejoy and Schertzer (2007) reviewed specifically that geofields (e.g., topography, turbulence, rock density and susceptibility, magnetic and gravitational fields) possess scale-invariance over wide range of scales. For instance, spectral analysis of rock susceptibilities showed a wide range of β-*values* ranging from 1 to 5, which enlightened the understanding of the fractal nature of magnetic sources within the crust (Pilkington and Todoeschuck, 1993; Maus and Dimri, 1994; Lovejoy et al., 2001). Although the mechanism of $1/f$ scaling

* Corresponding author.
E-mail addresses: chengxhg@163.com (G. Chen), qiuming@yorku.ca (Q. Cheng), zrguang@cug.edu.cn (R. Zuo).

http://dx.doi.org/10.1016/j.gexplo.2015.11.003
0375-6742/

nature of magnetization distribution remains unclear, it indeed facilitated the interpretation of magnetic data such as the depth determination of magnetic sources (Bouligand et al., 2009; Bansal and Dimri, 2014).

Based on multifractal theory, Cheng et al. (2000) have developed a spectrum–area (S–A) model to quantify the anisotropic scaling properties of geochemical and geophysical fields, which depict a generalized power-law relation between power spectrum and area of power spectrum exceeding a threshold. According to the S–A model, the isotropic 1/*f* scaling behavior in the frequency domain becomes a special case in which the scaling exponent can quantify some types of spatial association indexes (persistence, correlation, and roughness). In applied geochemistry, conventionally, the spatial variation (e.g., spatial correlation and variability within agent area) is quantified by autocorrelation and semivariogram, which has been widely taken into account in the spatial statistical methods for handling geochemical data (Cheng, 1999b; Agterberg, 2012a), such as moving average, kriging and spatial factor analysis. Accordingly, the scaling exponent (or fractal dimension) obtained from spectral method could provide an alternative approach to evaluate the spatial variation and quantify the scale invariance of geochemical variables from a fractal perspective.

To date, research intentions have not been given enough to explore the 1/*f* scaling natures of geochemical landscapes. This study is devoted to use scaling noise to model geochemical landscapes and to investigate the implication of scaling exponent (β) especially for geochemical anomalies associated with mineralization. We describe first the spectral method used to estimate the scaling exponent and fractal dimension of geochemical landscapes, then simulate fractal geochemical pattern aiming at understanding its scaling properties from fractal filtering point of view. Subsequently, a case study from the Nanling Range (China), which is endowed with abundant W–Sn mineral resources, help look at the diversity of 1/*f* scaling natures of real geochemical data, with a final intention to discuss the spatial association between fractal dimension and mineralization.

2. Methods

2.1. Fractal analysis

There exist several approaches to estimate the fractal dimension (D) for self-affine series (Cheng, 1999b; Malamud and Turcotte, 1999),

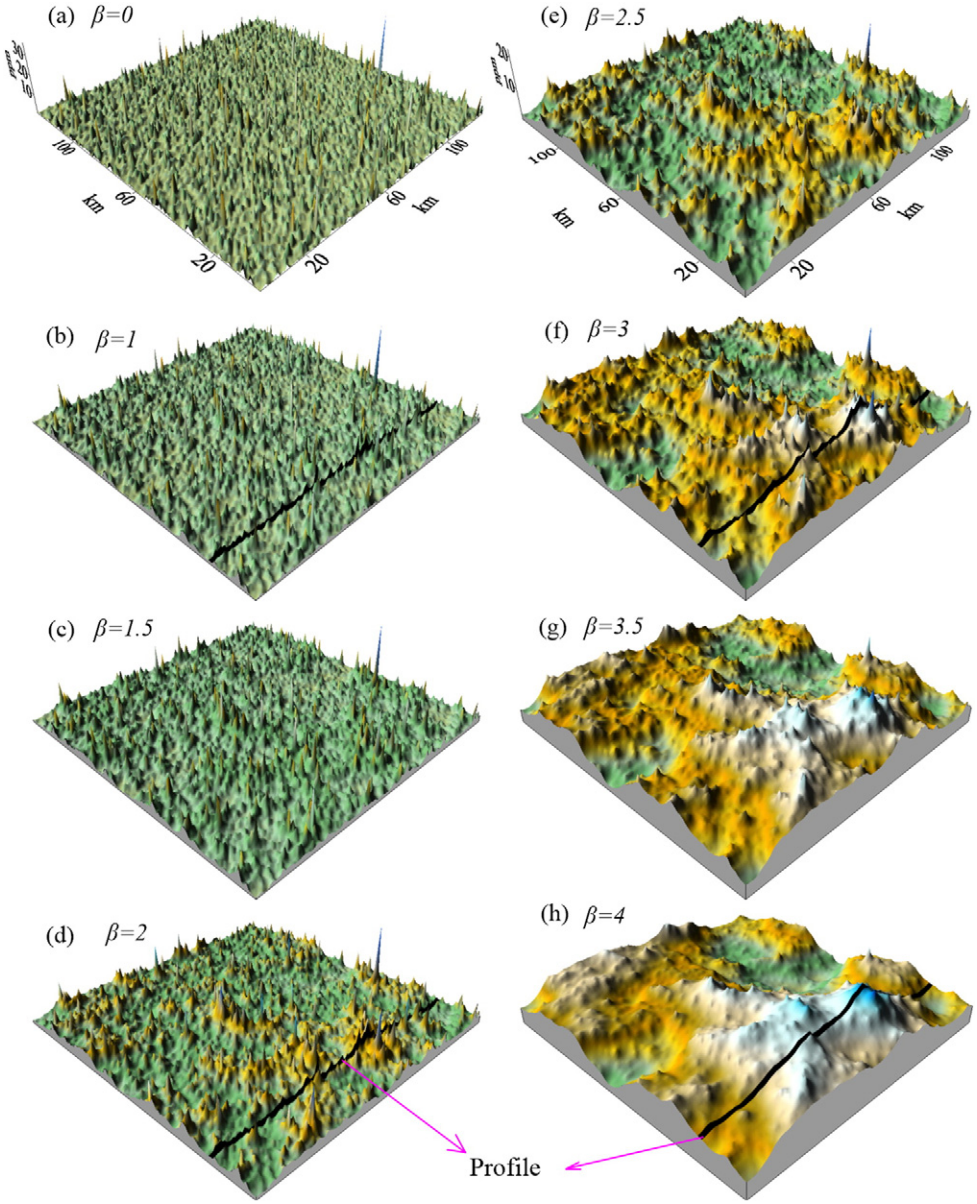

Fig. 1. Simulated fractal geochemical landscapes by using scaling filtering with different *β-values*: (a) 0, (b) 1, (c) 1.5,(d) 2, (e) 2.5, (f) 3, (g) 3.5 and (h) 4.

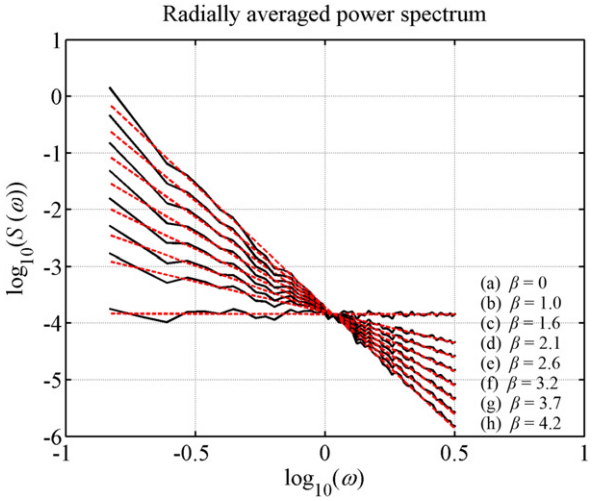

Fig. 2. Log–log plots of radially averaged power spectrum versus wavenumber for synthetic geochemical data in Fig. 1.

including spectral analysis, semivariogram, rescaled-range (R/S) analysis, correlation analysis and so on. Spectral method is the typical way to study the $1/f$ scaling law and respects relatively small biased results and low variance in estimating D (Schepers et al., 1992). We briefly recall herein the methodology of spectral method for estimating scaling exponent and fractal dimension. A two-dimensional (2D) data $f(x,y)$ can be Fourier transformed as:

$$F(\omega_x,\omega_y)=\sum_{x=0}^{N_x-1}\sum_{y=0}^{N_y-1} f(x,y)\exp\left[-\frac{i2\pi x\omega_x}{N_x}-\frac{i2\pi y\omega_y}{N_y}\right], \quad (1)$$

where $F(\omega_x,\omega_y)$ is the Fourier transformation coefficient of $f(x,y)$, $[N_x, N_y]$ is the size of $f(x,y)$ matrix, ω_x and ω_y denote the wavenumber in x- and y-directions, respectively. The power spectrum $F^2(\omega_x,\omega_y)$ of $f(x,y)$ can be written as:

$$F^2(\omega_r,\varphi)=F^2(\omega_r\cos\varphi,\omega_r\sin\varphi), \quad (2)$$

where $\omega_r=(\omega_x{}^2+\omega_y{}^2)^{1/2}$ is the radial wavenumber, and φ denotes the angle between radial direction and ω_x axis. Then the power density (radially averaged) spectrum $S(\omega_r)$ can be estimated as:

$$S(\omega_r)=\frac{1}{2\pi}\int_0^{2\pi}F^2(\omega_r,\varphi)d\varphi. \quad (3)$$

For a self-affine series, the radially averaged power spectrum has a power-law dependence on ω_r (Voss, 1988; Huang and Turcotte, 1989):

$$S(\omega_r)=c\omega_r^{-\beta} \quad (4)$$

where c is a constant value, and β is known as isotropic scaling exponent measuring the persistence or correlation between adjacent values within time series. When $\beta<0$, we have anti-correlated values of successive points; when $\beta=0$, the time series is completely uncorrelated (e.g., white noise); when $\beta>0$ and becomes more positive, the time series become more correlated.

The relationship between scaling exponent β and fractal dimension D given by Voss (1988) can be written as

$$D=(8-\beta)/2. \quad (5)$$

Fractal dimension (D) is a measure of surface roughness, representing the capability of the random variables to fill the Euclidean space. Theoretically, for a smooth 2D surface, the fractal dimension is $D\approx 2$ ($\beta\approx 4$), and for a rough surface, $2<D<3$ ($2<\beta<4$).

The scaling exponent β and fractal dimension D are both measures of persistence or roughness for self-affine objects. Malamud and Turcotte (1999) pointed out that semivariogram and R/S analysis are only applicable for measuring limited range of persistence (β), whereas spectral analysis can quantify all values of β. It must be noted that although the fractal dimension estimated from spectral method may be less than 2 or exceeds 3 in the practical 2D data analysis (see e.g., Huang and Turcotte, 1989; Turcotte, 1997) and the *D-value* seems to be meaningless for 2D topological space, it indeed acts as a quantification of persistence or roughness of self-affine objects.

2.2. Scaling filtering

The $1/f$ noise pattern can be generated synthetically using scaling (fractal) filtering method, which has been widely employed to model various scaling geofields such as topography (Turcotte, 1997), magnetic anomalies and magnetizations (Pilkington and Todoeschuck, 1993). Here, we propose to use the scaling filtering method to model geochemical landscapes with fractal properties. This process is summarized as follows. (1) The De Wijis cascade process (De Wijs, 1951) is exploited to produce a 2D dataset of geochemical concentration values which respect log-normal distribution. (2) These values are randomly distributed into white noise (Fig. 1a). (3) This white noise data are then transformed into Fourier domain with flat power spectrum (Fig. 2a) as expected. (4) The Fourier transformation coefficients are further multiplied by a scaling filtering function $\omega_r{}^{-\beta/2}$

$$F'(\omega_x,\omega_y)=\omega_r{}^{-\beta/2}F(\omega_x,\omega_y), \quad (6)$$

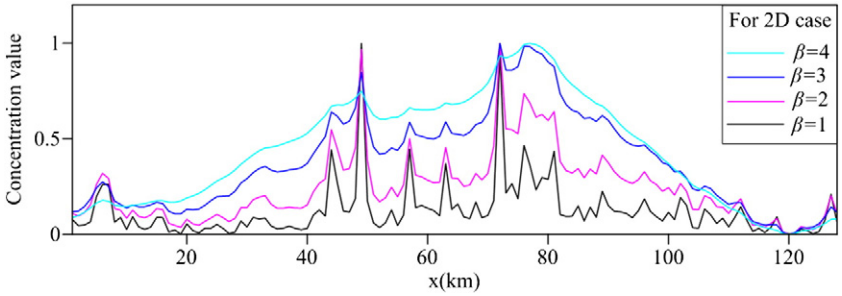

Fig. 3. Profile geochemical anomalies extracted from the synthetic 2D geochemical landscape in Fig. 1.

where β is the required scaling exponent. (5) The inverse Fourier transformation gives the fractal patterns yielding isotropic scaling (f^{β}) laws.

Here, the scaling exponents are specified as $\beta = 1$, 1.5, 2, 2.5, 3, 3.5, and 4 to generate fractal geochemical patterns (corresponding to Fig. 1b to h, respectively). The log–log plots of power density spectrum against wavenumber in Fig. 2 demonstrate that these patterns have been endowed with scaling properties, and their slopes are close to the desired β-*values*. From Fig. 1a to h as β-*value* increases in the low-pass scaling filtering function of Eq. (6), the geochemical landscape become smoother due to the reduction of high-frequency (irregular/stochastic) components, i.e., the enhancement of low-frequency (regular/deterministic) components. This fact also can be intuitively observed from the profile anomalies as illustrated in Fig. 3, where a bigger β-*value* produces a smoother geochemical curve with reducing irregularities/singularities.

In this sense, it can be appreciated the scaling exponent (β) conducts the fractal filtering by controling the balance of stochastic and deterministic components contained in geochemical patterns thereby determining the roughness. Specifically, $\beta = 0$ indicates a completely spatially uncorrelated geochemical pattern; $0 < \beta < 1$ indicates a highly random pattern with weak persistence and uncorrelated profile anomalies; and $\beta > 1$ indicates a spatially correlated pattern with growing persistence. As β-*value* increases to 4, the geochemical landscape (Fig. 1h) becomes a smooth surface with fractal dimension $D \approx 2$.

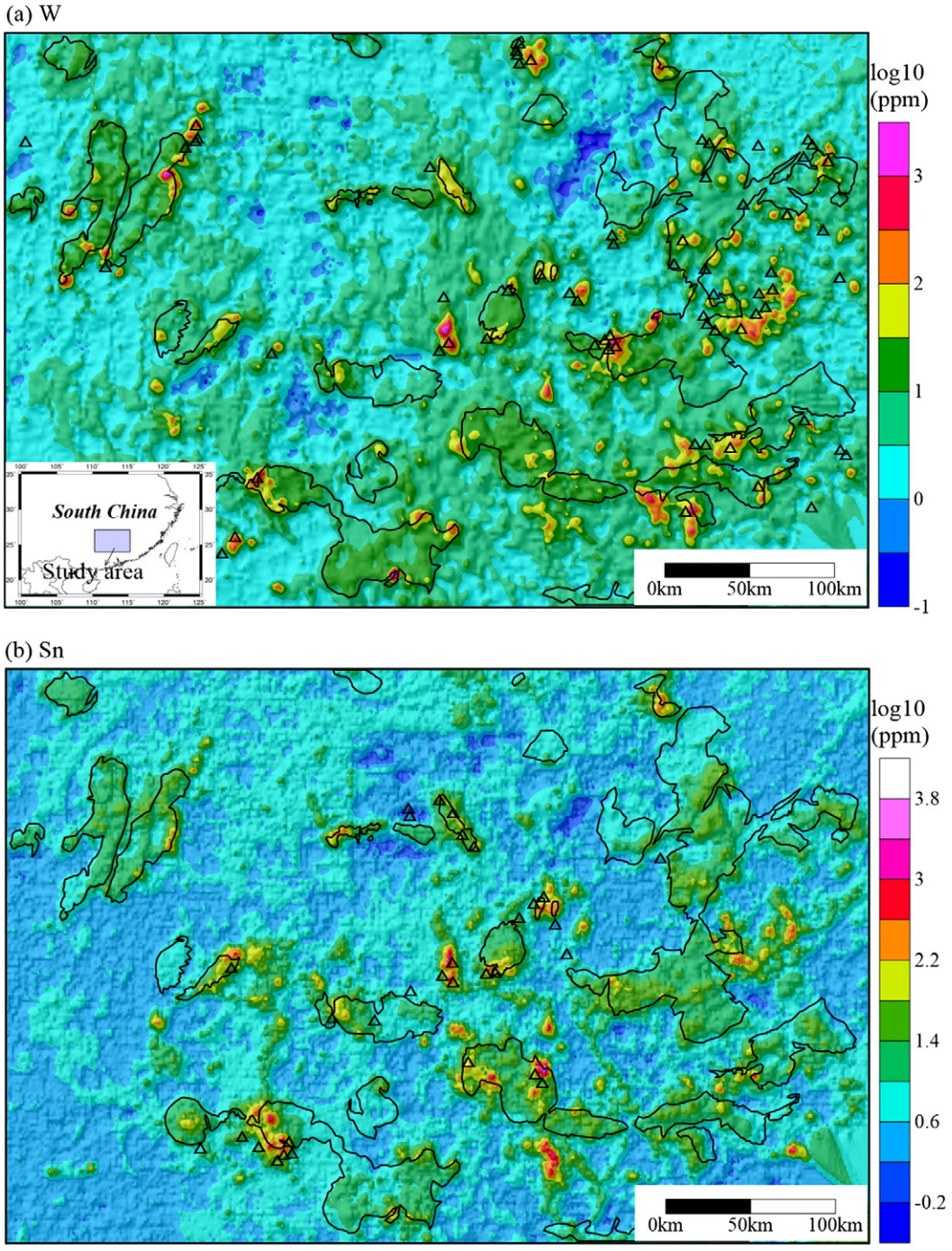

Fig. 4. Spatial distribution patterns of geochemical (a) W and (b) Sn elements (log10 (concentration value)). Triangular symbols indicate the locations of W or Sn deposits, and black lines show the boundaries of granites.

3. Study area and dataset

Nanling Range is geographically located in the intersecting area of Hunan, Jiangxi, Guangdong, and Guangxi provinces in the South China, with area over 180,000 km^2. Multiple tectonic events since Palaeozoic lead to the complicated geological settings including widespread magmatic activities with the outcropping granites area around 50,000 km^2. Highly enriched non-ferrous and rare minerals related to felsic intrusive rocks and low-temperature hydrothermal systems make this region the most famous and important polymetallic metallogenic provinces in China. The regional reserves of W and Sn ores account for approximately 83% and 63% of the total amounts of identified resources in China, respectively. Numerous world class W–Sn polymetallic deposits, such as Xihuashan W deposits, Shizhuyuan W–Sn–Mo–Bi, and Furong W–Sn, occurred alongside the granites during the Jurassic and Cretaceous. It is worth mentioning that Chinese scholar Yu (2011a, b, c) has done a great deal of pioneering studies for applying the complexity science (e.g., fractals, chaos and self-organized criticality) to study the formation and distribution of mineral deposit in the Nanling Range.

The samples used in this study were collected and analyzed during the Chinese National Geochemical Mapping (CNGM) project. Details of sampling and analysis of stream sedimentary geochemistry data can be found in Xie et al. (1997). Fig. 4 is the spatial distribution pattern of W and Sn elements with resolution of 2 km. In the last century, lognormal distribution is one of the basic assumptions in geochemical abundance models (Harris, 1984; Sinclair, 1991) even once acted as the first law of geochemical distribution (Ahrens, 1953). However, many studies suggest that, for trace elements, the large concentration values (geochemical anomaly) often satisfy extreme-value distributions (e.g., Pareto or fractal distribution) with a tail that is thicker than lognormal (Cheng et al., 1994; Agterberg, 2014b). Evidently, the Q–Q plots (Fig. 5) in this study show that W and Sn elements do not strictly follow lognormal distributions since the point dots depart from the lognormal straight lines. The frequency distribution (histogram in Fig. 5) of these trace elements (e.g., W and Sn) concentration values often has high-value tails that are thicker and longer than lognormal tails, suggesting that the geochemical concentrations of W and Sn may follow the fractal statistical distributions, but it make no sense to the spatial correlation. In subsequent sections, a special intention is devoted, from scaling ($1/f$) noise point of view, to explore the fractal natures of geochemical patterns concerning with roughness.

4. Scaling natures of geochemical landscape

This section aims to explore the $1/f$ scaling natures of geochemical landscapes in Nanling Range, including trace elements (e.g., W, Sn, Mo, Bi, Pb, Zn, Au, Ag and Cu) and major elements (e.g., K_2O, Na_2O, CaO, Fe_2O_3 and SiO_2). Their individual power density spectra at all scales (wavenumbers) are first calculated. Fig. 6 just shows the log–log plots of selected elements (viz., W, Sn, Mo, Au, K_2O and Fe_2O_3) well fitted by straight lines, suggesting that geochemical landscapes exhibit frequency-independent spectrum, i.e., fractal or at least scaling natures. Then the global scaling exponent or "structural" fractal dimension can be estimated from the slope of the fitted straight lines in Fig. 6.

The estimated global scaling exponent of geochemical landscapes ranges from 1.22 to 2.64 (Table 1). Zn element holds the lowest β-*value* while K_2O has the highest. Major elements generally possess larger β-*value* ($2.13 \le \beta \le 2.82$) than that of trace elements ($1.22 \le \beta \le 1.85$), since the formers generally are distributed relatively homogeneously within the Earth' crust. In addition, there are explicit differences in β-*values* between highly enriched elements and relatively low enriched elements in the study area (Table 1). The selected enriched elements (e.g., W, Sn, Mo, Bi and Pb) show scaling exponent $\beta \approx 1.8$ and

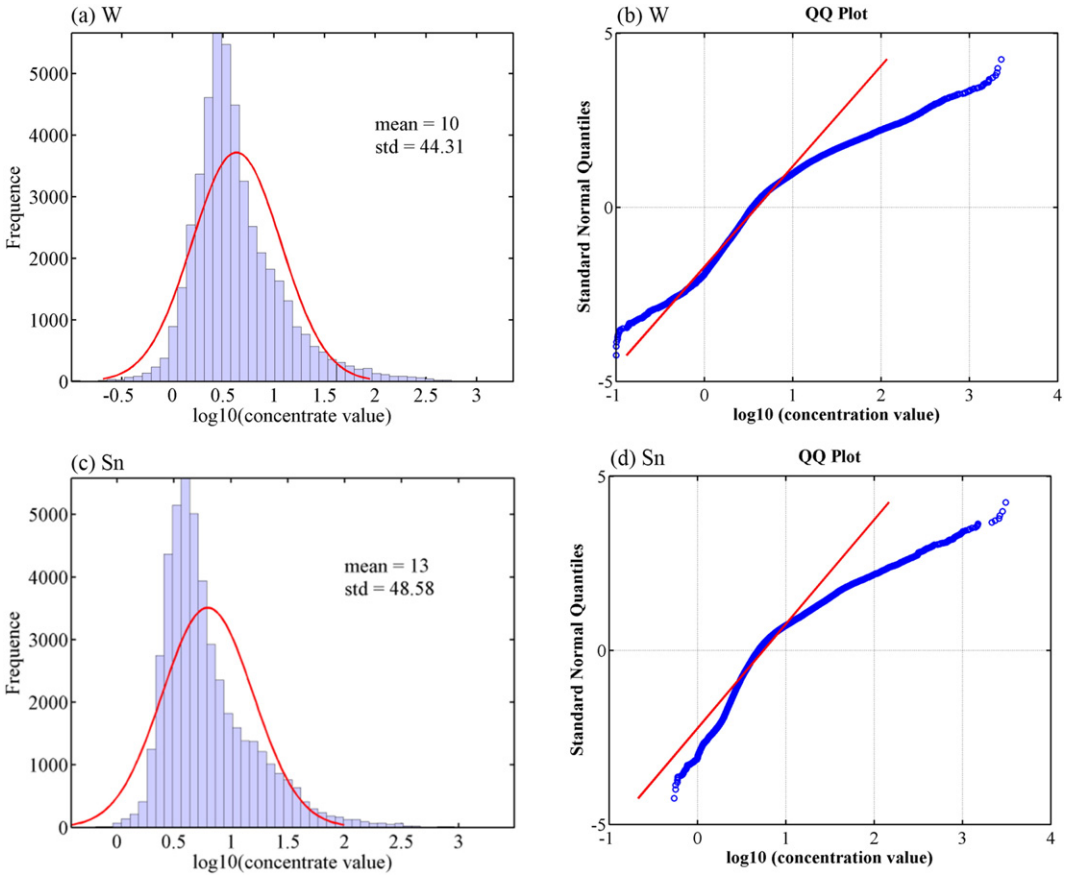

Fig. 5. Histograms of (a) log-transformed W and (c) log-transformed Sn. Q–Q plots of (b) log-transformed W and (d) log-transformed Sn.

(structural) fractal dimension $D \approx 3.1$, indicating that their geochemical patterns contain lots of irregularities/singularities. Those relatively lowly enriched elements (e.g., Au, Ag and Cu) have smaller scaling exponent ($\beta \approx 1.5$, $D \approx 3.3$), suggesting that they contain more stochastic components than the enriched elements. These results demonstrate that geochemical landscapes manifest diverse scaling (f^{β}) rules, and the scaling exponent (or fractal dimension) measures the roughness, i.e., the proportion of irregular and regular components contained in the geochemical patterns.

What do fractals come from? Numerous mechanisms (e.g., nesting and self-organized criticality) have been proposed for leading scale invariance but none of them can explain the whole nature (Hergarten, 2002). The simplest mechanism explains fractals as a product of other fractal/multifractal system. From fractal filtering point of view, the scaling natures of geochemical landscapes may be roughly seen as the end products of the complex compeling geo-process (e.g., tectonic activities, bedrock lithologies, weathering process, topography, and presence of mineral deposits) that may converts chaotic inputs

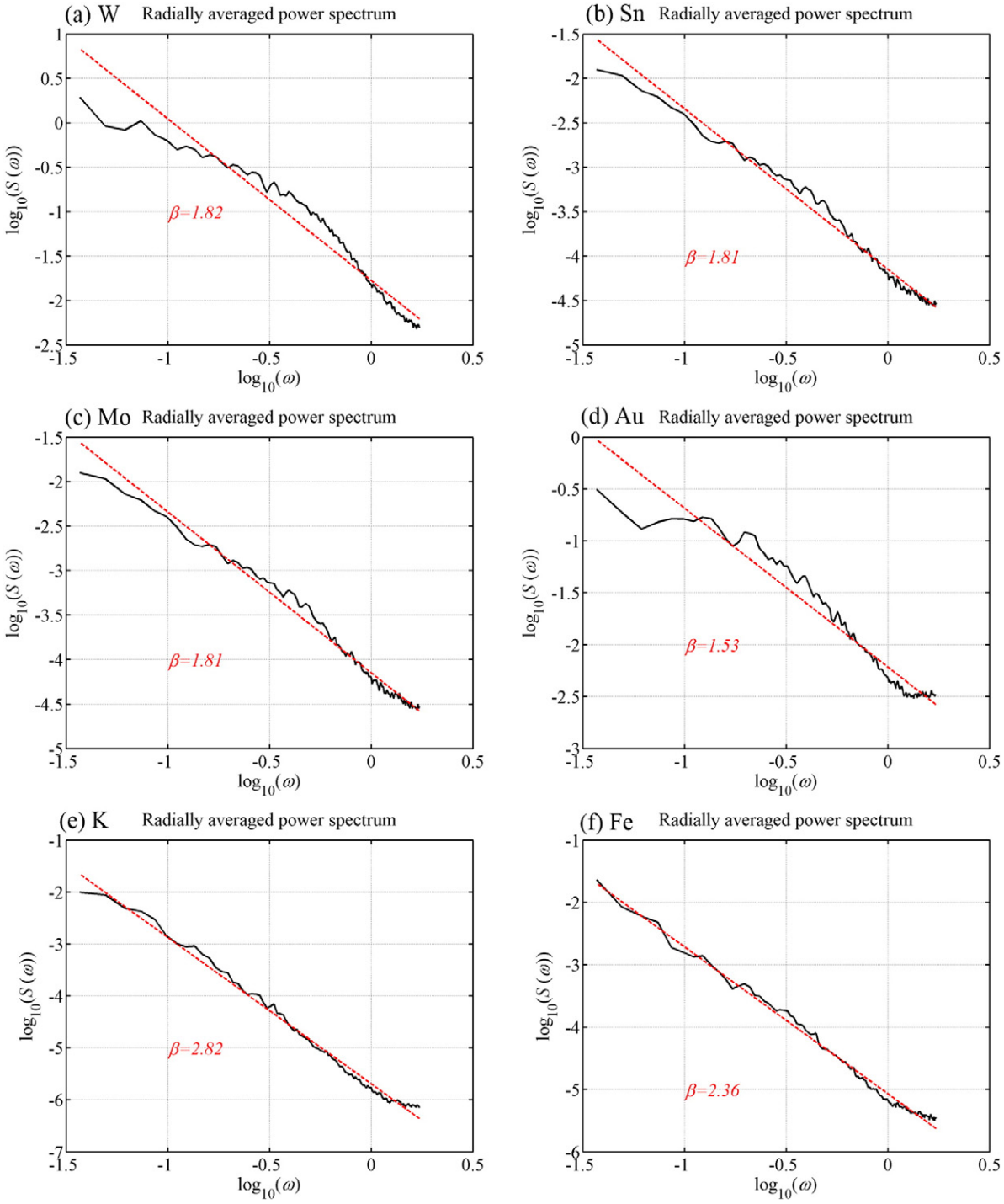

Fig. 6. Log–log plots of radially averaged power spectrum versus wavenumber for geochemical data (without log-transform), including trace elements (a) W, (b) Sn, (c) Mo, (d) Au, and major elements (e) K_2O and (f) Fe_2O_3.

Table 1
Scaling exponents and fractal dimensions estimated from the stream sedimentary geochemical landscapes in the Nanling Range.

Elements	Scaling exponent (β)	Fractal dimension (D)
W	1.82	3.09
Sn	1.82	3.09
Mo	1.81	3.10
Bi	1.85	3.08
Pb	1.84	3.07
Zn	1.22	3.39
Au	1.53	3.24
Ag	1.34	3.33
Cu	1.52	3.24
K_2O	2.82	2.59
Na_2O	2.64	2.68
CaO	2.13	2.94
Fe_2O_3	2.36	2.82
SiO_2	2.44	2.78

into $1/f^{\beta}$ scaling outputs. Different geo-processes may act as different fractal filters with specific scaling exponent (β), which are certainly various for multiple elements, and result in diverse scaling distributions of metal elements. In general, the geo-process contains both stochastic and deterministic factors (Cheng, 1999a), so the geochemical landscape does (Walther, 2009; Agterberg, 2012a). Both stochastic (irregular) and deterministic (regular) components in geochemical patterns are crucial for indicating mineralization. Deterministic components often describe the trend (background) of geochemical pattern, while stochastic components determine the local discontinuities (anomalies). The mineral deposits often generate distinct geochemical anomalies at local scale accompanied by significant geochemical background/province. Such backgrounds generally correspond to specific geological settings which could provide abundant sources for the formation of mineralization. For instance, most of the W and Sn deposits in Nanling Range are accompanied with local geochemical anomalies (Fig. 4),

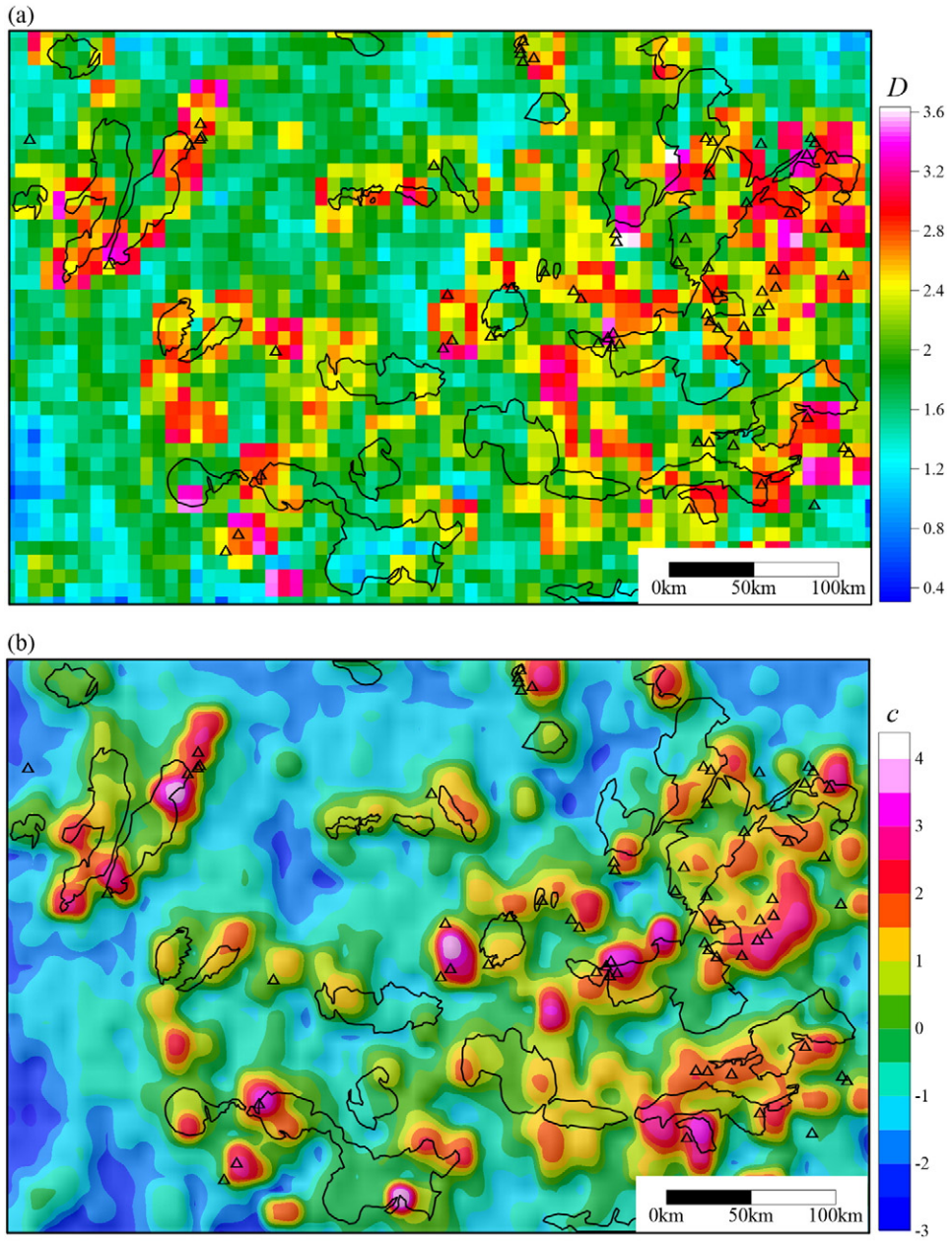

Fig. 7. Fractal mapping results of W element in the Nanling Range using window-based method. (a) 2D spatial distribution of local fractal dimensions, (b) 2D spatial distribution of estimated constant value.

while these anomalies are superposed on the background of elevated geochemical concentrations whose framework indicates granitic intrusions. In addtion, we infer that the scaling exponent of geochemical anomalies pattern mainly ranges from 1 to 4, implying a weak balance of stochastic and deterministic components.

5. Fractal mapping of geochemical anomaly

Geochemical patterns respect various global scaling natures which reflect the scale-dependent spatial variations (persistence/correlation/roughness). This scaling behavior appears to vary spatially in light of the widely used singularity mapping (LSA) method, so fractal mapping is undertaken to look at the regional-dependent variation of local fractal dimension and to investigate its spatial association with mineralization. A window-based method has already been introduced by Huang and Turcotte (1989) to estimate the local fractal dimension of topography. Here, this approach is used to handle 2D geochemical data. The procedure is summarized as: (1) Define a square window $A(\varepsilon)$ with window sizes ε for a given sampling point on the map. (2) Take Fourier transformation of geochemical data within the window, and calculate the radially averaged power spectrum $S(\omega_r)$. (3) The scaling exponent (β) and constant value (c) can be calculated based on the slope of radial average

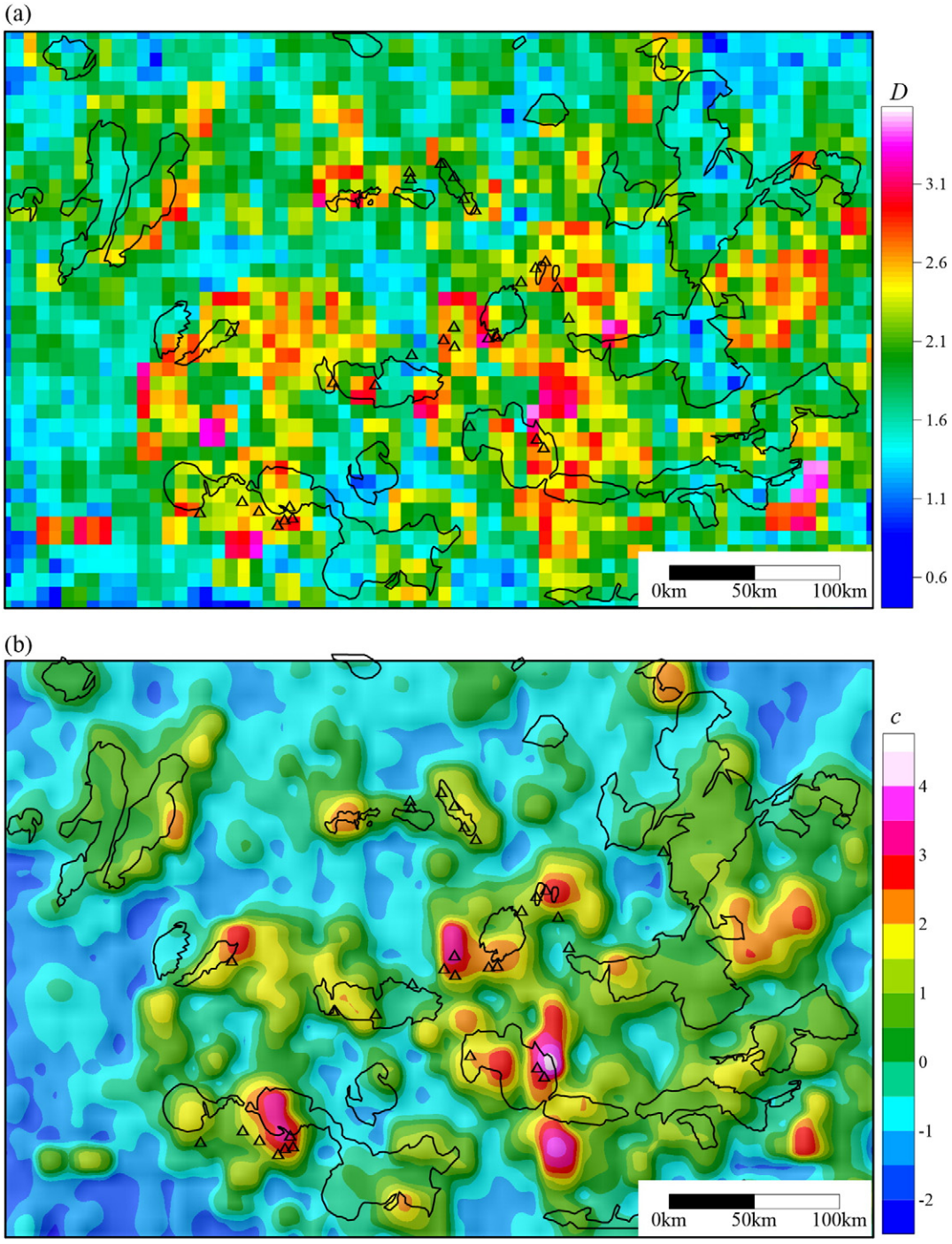

Fig. 8. Fractal mapping result of Sn element in the Nanling Range using window-based method. (a) 2D spatial distribution of local fractal dimensions, (b) 2D spatial distribution of estimated constant value.

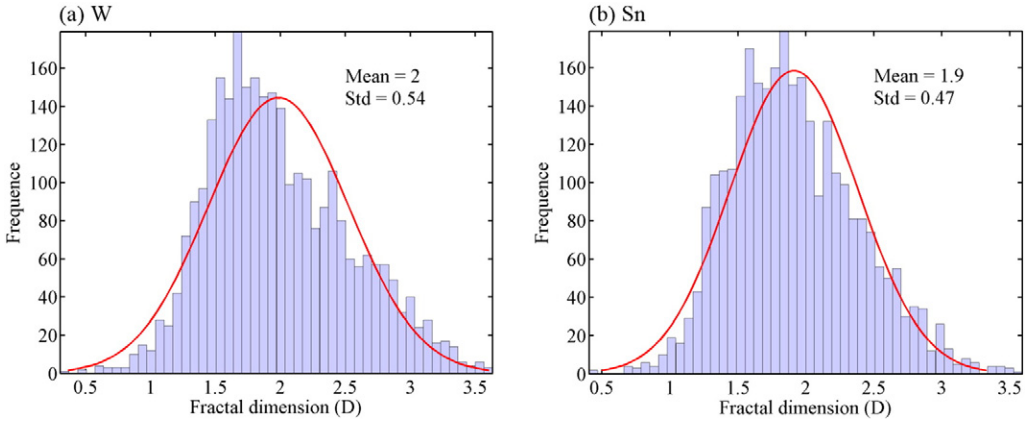

Fig. 9. Histogram statistic on estimated local fractal dimensions in Figs. 7a and 8a.

power spectrum in log–log space. (4) Estimate the fractal dimension D based on Eq. (5). (5) Construct the spatial distribution of local fractal dimension (D) and constant value (c) based on a moving window method.

Since the Nanling Range hosts a number of W–Sn polymetallic deposits, W and Sn elements (Fig. 4) are chosen to study fractal mapping result. It should be emphasized that different window sizes can result in different spatial resolutions of fractal dimension patterns, and using small widow size obtains subtle information but increases the errors in the calculation. We carried out tests of using various window sizes (e.g., 8 km × 8 km, 16 km × 16 km, 32 km × 32 km and 64 km × 64 km), and chose the production of 16 km × 16 km because of its rich details and reliable goodness of fitting. Figs. 7 and 8 correspond to fractal dimension (D) and constant (c) map, respectively. The histogram in Fig. 9a shows that *D-value* of W element ranges from 0.5 to 3.5, *mean* = 2.0 and standard deviation = 0.55. Analogously, the *D-value* of Sn element ranges from 0.5 to 3.5, *mean* = 1.9 and standard deviation = 0.48 (Fig. 9b). W and Sn elements have similar statistic on fractal dimensions (or scaling exponent) since they are often coexisted in the W–Sn deposits in Nanling district.

Most of *D-values* in Figs. 7a and 8a surround the topological dimension $D = 2$, indicating that these subregions correspond to smooth background with few irregularities/singularities, while $D > 2$ ($\beta < 4$) indicates that irregular/singular components have been superposed on the regular background field. In some literatures (Agterberg, 2012b, 2012a; Cheng, 2012), special attentions have been paid to such irregularities/singularities arising from the mineralization which often assembled huge metals. Such singularity degree can be obtained from LSA for indicating the enrichment or deficit of elements and show close spatial connections with ore deposits (see e.g. Cheng and Agterberg, 2008; Zuo et al., 2009). Accordingly, the spatial variation of local fractal dimension can imply the contribution of irregularities/singularities in geochemical pattern, which may exhibit potential associations with mineralization.

We superposed the locations of known W and Sn deposits on Figs. 7 and 8 to reveal the spatial relationship between local fractal dimension and mineralization. Cursory visual inspection of Figs. 7 and 8 suggests that most of the W and Sn deposits are located in the areas with relatively high fractal dimension. We extracted the *D-values* in the subregions hosting mineral deposits, and their boxplots in Fig. 10 suggest that *D-value* for W and Sn deposits ranges from 2.4 to 2.7 and 2.3 to 2.7, respectively. This result suggests that the geochemical anomalies associated with mineralization exhibit rough signatures which possess scaling exponent in the range $1 < \beta < 4$. In addition, Figs. 7b and 8b show the mapping results of constant value and contain regional components of geochemical field, presenting distinct patterns related to the distribution of granitic outcrops.

6. Conclusions

The scaling noise was proposed to model and analyze geochemical landscapes in this contribution. The 1/*f* scaling natures of geochemical distribution of multiple elements were explored using a case study of Nanling Range (China). The results showed that (1) the global scaling exponent ranges from 1.22 to 2.64 for geochemical distribution; and (2) most of W–Sn deposits occur in (or near) areas linked to relatively high dimension value ($2.3 \le D \le 2.7$). These findings suggested that geochemical landscapes manifest 1/*f* scaling natures which reflect the spatial variations (persistence and roughness), and we provided a fractal

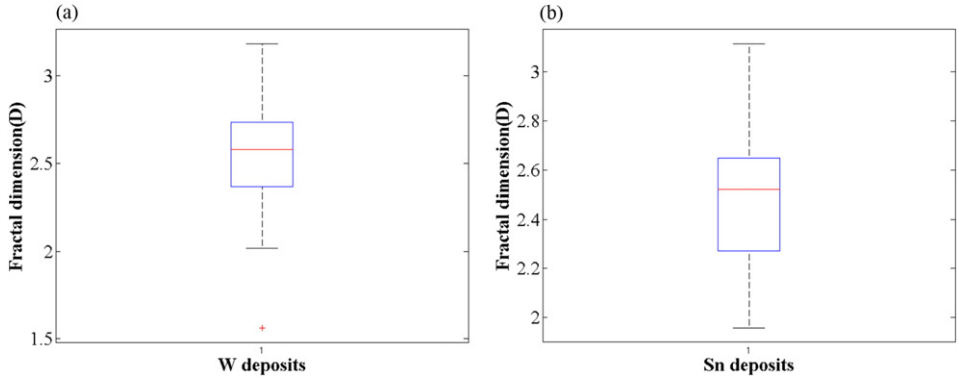

Fig. 10. Boxplots of estimated fractal dimensions within the subregions of (a) W deposits and (b) Sn deposits.

point view for recognizing the complexity of geochemical anomalies related to mineralization containing both regular and irregular components.

The results in this paper can be regarded as a preliminary investigation. There is much work to be done both experimentally and theoretically before we can really understand the physical processing driving these 1/*f* scaling systems. More case studies from various geological settings would better define the scaling natures of geochemical landscapes and offer deeper insights into the process statistics of near-surface variability of metal elements. In addition, the 1/*f* noise is often associated with chaos and self-organized criticality (SOC). It may be promising to integrate the chaos/SOC theories and the 1/*f* scaling process to study whether/how metal elements (self-) organize to form mineral deposits as the end product of complex geo-process or chaotic dynamic system containing both deterministic and stochastic factor.

Acknowledgments

Thanks are due to the helpful discussions with Prof. Christian Haas and Dr. Jiangtao Liu. This work benefits from the joint support by a National Natural Foundation of China (No. 41430320), a research project from China Geology Survey (No. 12120113089000), excellent PhD thesis funding from China University of Geosciences Wuhan and a special student fund project (WHS201311) from IGGE.

References

Afzal, P., Alghalandis, Y.F., Khakzad, A., Moarefvand, P., Omran, N.R., 2011. Delineation of mineralization zones in porphyry Cu deposits by fractal concentration–volume modeling. J. Geochem. Explor. 108, 220–232.
Afzal, P., Ahari, H.D., Omran, N.R., Aliyari, F., 2013. Delineation of gold mineralized zones using concentration–volume fractal model in Qolqoleh gold deposit, NW Iran. Ore Geol. Rev. 55, 125–133.
Agterberg, F., 2012a. Multifractals and geostatistics. J. Geochem. Explor. 122, 113–122.
Agterberg, F., 2012b. Sampling and analysis of chemical element concentration distribution in rock units and orebodies. Nonlinear Process. Geophys. 19, 23–44.
Agterberg, F., 2014a. Geomathematics: Theoretical Foundations. Springer, Applications and Future Developments.
Agterberg, F., 2014b. Geomathematics: theoretical foundations, applications and future developments. Quantitative Geology and Geostatistics vol. 18. Springer.
Ahrens, L., 1953. A fundamental law of geochemistry. Nature 172, 1148.
Bansal, A., Dimri, V., 2014. Modelling of magnetic data for scaling geology. Geophys. Prospect. 62, 385–396.
Bouligand, C., Glen, J.M., Blakely, R.J., 2009. Mapping Curie temperature depth in the western United States with a fractal model for crustal magnetization. J. Geophys. Res. 114, B11104.
Cheng, Q., 1999a. Multifractality and spatial statistics. Comput. Geosci. 25, 949–961.
Cheng, Q., 1999b. Spatial and scaling modelling for geochemical anomaly separation. J. Geochem. Explor. 65, 175–194.
Cheng, Q., 2006. GIS-based multifractal anomaly analysis for prediction of mineralization and mineral deposits. In: Harris, J. (Ed.), GIS Applications in Earth Sciences, Geological Association of Canada, pp. 289–300.
Cheng, Q., 2007. Mapping singularities with stream sediment geochemical data for prediction of undiscovered mineral deposits in Gejiu, Yunnan Province, China. Ore Geol. Rev. 32, 314–324.
Cheng, Q., 2008. Non-linear theory and power-law models for information integration and mineral resources quantitative assessments. Math. Geosci. 40, 503–532.
Cheng, Q., 2012. Singularity theory and methods for mapping geochemical anomalies caused by buried sources and for predicting undiscovered mineral deposits in covered areas. J. Geochem. Explor. 122, 55–70.
Cheng, Q., Agterberg, F.P., 2008. Singularity analysis of ore-mineral and toxic trace elements in stream sediments. Comput. Geosci. 35, 234–244.
Cheng, Q., Agterberg, F., Ballantyne, S., 1994. The separation of geochemical anomalies from background by fractal methods. J. Geochem. Explor. 51, 109–130.
Cheng, Q., Xu, Y., Grunsky, E., 2000. Integrated spatial and spectrum method for geochemical anomaly separation. Nat. Resour. Res. 9, 43–52.
Chen, G., Cheng, Q., Zuo, R., Liu, T., Xi, Y., 2015. Identifying gravity anomalies caused by granitic intrusions in Nanling mineral district, China: a multifractal perspective. Geophys. Prospect. 63, 256–270.
De Wijs, H., 1951. Statistics of ore distribution. Part I: frequency distribution of assay values. J. R. Neth. Geol. Mining Soc. 13, 365–375.
Harris, D.P., 1984. Mineral Resources Appraisal: Mineral Endowment, Resources, and Potential Supply: Concepts, Methods and Cases. Oxford University Press, New York.
Hergarten, S., 2002. Self Organized Criticality in Earth Systems. Springer.
Huang, J., Turcotte, D., 1989. Fractal mapping of digitized images: application to the topography of Arizona and comparisons with synthetic images. J. Geophys. Res. Solid Earth 94, 7491–7495 (1978–2012).
Li, C., Ma, T., Shi, J., 2003. Application of a fractal method relating concentrations and distances for separation of geochemical anomalies from background. J. Geochem. Explor. 77, 167–175.
Lovejoy, S., Schertzer, D., 2007. Scaling and multifractal fields in the solid earth and topography. Nonlinear Process. Geophys. 14, 465–502.
Lovejoy, S., Pecknold, S., Schertzer, D., 2001. Stratified multifractal magnetization and surface geomagnetic fields—I. Spectral analysis and modelling. Geophys. J. Int. 145, 112–126.
Malamud, B.D., Turcotte, D.L., 1999. Self-affine time series: measures of weak and strong persistence. J. Stat. Plan. Infer. 80, 173–196.
Mandelbrot, B., 1967. How long is the coast of Britain. Science 156, 636–638.
Mandelbrot, B., 1989. Multifractal measures, especially for the geophysicist. Pure Appl. Geophys. 131, 5–42.
Maus, S., Dimri, V., 1994. Scaling properties of potential fields due to scaling sources. Geophys. Res. Lett. 21, 891–894.
Pilkington, M., Todoeschuck, J., 1993. Fractal magnetization of continental crust. Geophys. Res. Lett. 20, 627–630.
Schepers, H.E., Van Beek, J.H., Bassingthwaighte, J.B., 1992. Four methods to estimate the fractal dimension from self-affine signals (medical application). Eng. Med. Biol. Mag. IEEE 11, 57–64.
Sinclair, A., 1991. A fundamental approach to threshold estimation in exploration geochemistry: probability plots revisited. J. Geochem. Explor. 41, 1–22.
Turcotte, D.L., 1997. Fractals and Chaos in Geology and Geophysics. Cambridge university Press.
Voss, R.F., 1988. Fractals in Nature: From Characterization to Simulation. Springer.
Walther, J.V., 2009. Essentials of Geochemistry. Jones & Bartlett Publishers.
Xie, X., Mu, X., Ren, T., 1997. Geochemical mapping in China. J. Geochem. Explor. 60, 99–113.
Yu, C., 2011a. The characteristic target-pattern regional ore zonality of the Nanling region, China (I). Geosci. Front. 2, 147–156.
Yu, C., 2011b. The characteristic target-pattern regional ore zonality of the Nanling region, China (II). Geosci. Front. 2, 323–347.
Yu, C., 2011c. The characteristic target-pattern regional ore zonality of the Nanling region, China (III). Geosci. Front. 2, 551–569.
Zuo, R., Cheng, Q., Agterberg, F., Xia, Q., 2009. Application of singularity mapping technique to identify local anomalies using stream sediment geochemical data, a case study from Gangdese, Tibet, western China. J. Geochem. Explor. 101, 225–235.